

# **Investigation of atmospheric and hydrological loading signals in the annual signal of GPS station positions**

**Sofiane KHELIFA, Algeria**

**Key words:** GPS station positions, time series analysis, atmospheric loading, hydrological loading.

## **SUMMARY**

The purpose of the present study is to investigate the potential origin of the annual signal observed in GPS (Global Positioning System) station position time series by studying its correlation with the atmospheric and hydrological pressure loading signals. The data used are the daily position time series of 11 well-distributed GPS stations, referred to ITRF2014 and expressed in the local frame (North, East and Up). For the time series of displacements (North, East and Up) caused by the atmospheric and hydrological pressure loadings at the 11 selected sites, we used those estimated from the atmospheric models ECMWF-IB, ECMWF-TUGO-m barotropic and ERA interim, and from the hydrological models GLDAS/Noah, ERA interim and MERRA2.

The results reveal that the amplitudes average of the extracted annual signal in respectively, North, East and Up components is about of 0.55, 0.54 and 1.70 mm. The calculated correlations between the extracted annual signal and the atmospheric and hydrological loading displacements estimated from all used models, are small in the three components (North, East and Up) for all analyzed stations.

# Investigation of atmospheric and hydrological loading signals in the annual signal of GPS station positions

Sofiane KHELIFA, Algeria

## 1. INTRODUCTION

Space geodesy is the science which uses the satellite measurements to determine the shape of the Earth and its dimensions, as well as its gravity field. The developments of space geodesy allowed the establishment of world geodetic networks observing constellations of satellites permanently. GPS (Global Positioning System) (Dow et al., 2009) is one of these permanent systems, as Very Long Baseline Interferometry (VLBI) (Schuh and Behrend, 2012), Satellite Laser Ranging (SLR) (Pearlman et al., 2002) and Doppler Orbitography and Radio-positioning Integrated by Satellite (DORIS) (Barlier, 2005). The various measurements derived from these systems (VLBI, SLR, GPS and DORIS) are collected, pre-processed and assigned a measurement date, we thus form time series.

The estimated coordinates of space geodetic stations (VLBI, SLR, GPS and DORIS) are now available in terms of time series with a sampling rate of one day to one week. These time series contain a considerable amount of information on geophysics (local movement of stations) but they are affected by noise and systematic errors (trend and seasonal terms) (Khelifa, 2016). The assessment of these residual errors in geodetic time series is essential to provide a better understanding of the physical phenomena governing the movement of the Earth's crust (movement of tectonic plates, geocenter variations, load effects, etc.), and to improve continually the accuracy of the estimated coordinates (Khelifa, 2016).

Many studies have demonstrated the presence of atmospheric and hydrological pressure loading in station coordinate time series (Petrov and Boy, 2004; Steigenberger et al., 2009; Eriksson and MacMillan, 2014). In this fact, we tried from this work to investigate the potential origin of the annual signal in GPS station coordinate time series by studying its correlation with atmospheric and hydrological pressure loading signals. For this purpose, we calculated the correlation between the annual signal in positions time series of 11 well-distributed GPS stations, and the three-dimensional displacements (North, East and Up) caused by atmospheric and hydrological loading for each analyzed station.

The discrete wavelet transform (multi-resolution analysis) is applied to assess the annual signal present in the GPS position time series. This method allows to study the signal at different resolutions using functions (called wavelets) well localised in both, the time and frequency domain, generated from each other by translation and dilation. The followed section provides a brief overview on the mathematical definitions of this method. For more details about this method, the reader is referred to (Daubechies, 1992; Mallat, 1999).

## 2. WAVELET TRANSFORMS

### 2.1 Continuous wavelet transform

The Continuous Wavelet Transform (CWT) of a signal  $X(t)$  can be expressed with the following equation (Daubechies, 1992; Mallat, 1999; Khelifa, 2016):

$$CWT_{u,s}(t) = \int_{-\infty}^{+\infty} X(t) \bar{\psi}_{u,s}(t) dt \quad (1)$$

$$\psi_{u,s}(t) = s^{-\frac{1}{2}} \psi\left(\frac{t-u}{s}\right) \text{ with } s \in \mathbb{R}_+^* \text{ and } u \in \mathbb{R} \quad (2)$$

Where  $u$  and  $s$  denote, respectively, the translation and scale factor, and  $\bar{\psi}_{u,s}$  denotes the complex conjugate of the wavelet functions  $\psi_{u,s}$ .

The original signal can be reconstructed from its wavelet coefficients  $CWT_{u,s}$  by the inverse wavelet transform (Daubechies, 1992; Mallat, 1999):

$$X(t) = \frac{1}{C_\psi} \int_0^{+\infty} \int_{-\infty}^{+\infty} CWT_{u,s}(t) \psi_{u,s}(t) du \frac{ds}{s^2} \quad (3)$$

$$C_\psi = \int_0^{+\infty} \frac{|FT(\psi(t))|^2}{t} dt \quad (4)$$

Where  $C_\psi$  denotes the admissibility constant and  $FT$  is the Fourier Transform. For a successful inverse wavelet transform, the admissibility constant has to check the admissibility condition:  $0 < C_\psi < +\infty$  (Daubechies, 1992; Mallat, 1999).

### 2.2 Discrete wavelet transform (multi-resolution analysis)

The Discrete Wavelet Transform (DWT) is obtained by sampling the wavelet function  $\psi$  at discrete translations and scales as follow (Daubechies, 1992; Khelifa, 2016):

$$s = s_0^j \text{ and } u = k u_0 s_0^j \text{ with } k, j \in \mathbb{Z}, s_0 > 1 \text{ and } u_0 > 0$$

$$\psi_{j,k}(t) = s_0^{-\frac{j}{2}} \psi\left(\frac{t - k u_0 s_0^j}{s_0^j}\right) \quad (5)$$

$$DWT_{j,k}(t) = s_0^{-\frac{j}{2}} \int_{-\infty}^{+\infty} X(t) \bar{\psi}(s_0^{-j} t - k u_0) dt \quad (6)$$

By varying the scale and translation factors in dyadic way (i.e., powers of two) by choosing  $s_0=2$  and  $u_0=1$ , leads to a multi-resolution analysis (MRA) (Mallat, 1999). The MRA approach allows to decompose a signal on several scales (resolutions) and to reconstruct it from the elements of this decomposition. At each scale, the original signal is decomposed into two signals: (i) the detail signal (representing its high frequencies), allows to assess the seasonal variability of the data, and (ii) the approximation signal (representing its low

frequencies), allows to identify the low-frequency variability events (trend) in time scale. Fig. 1 shows the scheme of multi-resolution analysis, in which a signal is decomposed into signals of approximation and detail in successive levels.

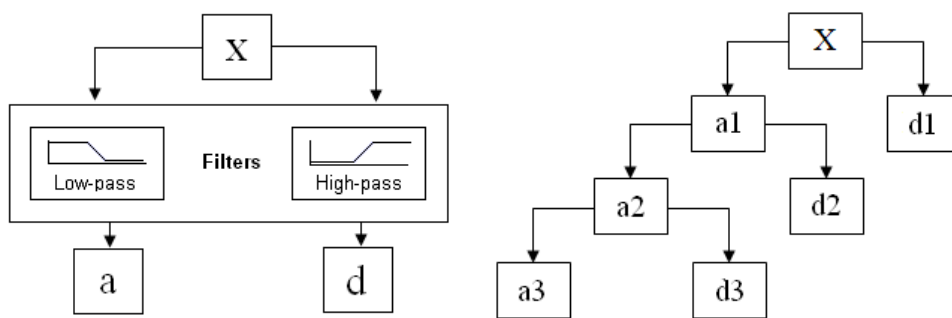


**Fig. 1.** Filtering process of multi-resolution analysis: the original signal X passes through two complementary filters (low-pass and high-pass filters) and emerges as two signals: approximation (a) and detail (d). In right graph, three levels of decomposition are shown.

### 3. DATA USED

For this study, we have used time series of daily position residuals of 11 GPS stations (see table 1) available on the JPL Web site (<http://sideshow.jpl.nasa.gov>). These data are computed by the JPL (Jet Propulsion Laboratory) Analysis Centre, using the precise point positioning strategy in the GIPSY/OASIS II software (Zumberge et al., 1997), referred to ITRF2014 (Altamimi et al., 2016) and expressed in the local geodetic reference frame (North, East and Up).

Acronym	Site	Country	Lat (deg)	Long (deg)	Data span
GODE	Greenblet	U.S.A.	38.90	-76.80	2013.0–2017.7
KOKB	Kauai	U.S.A. (Hawaii)	22.01	-159.67	2002.8–2017.7
METS	Metsahovi	Finland	60.20	24.70	1994.0–2017.7
NKLG	Libreville	Gabon	0.30	9.70	2011.4–2017.7
NYA1	Ny-Alesund	Norway	78.93	11.87	1998.2–2017.7
REYK	Reykjavik	Island	64.15	-21.98	1996.1–2017.7
STJO	St John's	Canada	47.60	-52.70	1994.0–2017.7
SYOG	Syowa	Antarctica	-69.00	39.58	1999.1–2017.7
THTI	Papeete	France	-17.58	-149.62	1999.5–2017.7

TLSE	Toulouse	France	43.55	1.48	2001.0–2010.2
USNO	Goldstone	U.S.A.	35.30	-116.80	2002.8–2017.7

**Table 1** GPS sites selected in this study.

## 4. RESULTS AND DISCUSSION

### 4.1 Annual signal

Seasonal signals contained in the analyzed time series can be identified by the detail signals derived from the multi-resolution analysis. The annual signals in the analyzed position time series have been identified with the detail signal at level 8 (detail 8). Fig. 2 shows an example of the annual signal extracted from the Up component of NKLG station. The annual amplitudes of the three components (North, East and Up) for the analyzed position time series are given in Table 2. The Average annual amplitude is about of 0.55, 0.54 and 1.70 mm in the components North, East and Up, respectively.

Stations	North (mm)	East (mm)	Up (mm)
GODE	0.50	0.46	1.39
KOKB	0.60	0.48	1.32
METS	0.66	0.47	1.28
NKLG	0.68	0.78	1.95
NYA1	0.48	0.45	1.50
REYK	0.37	0.70	1.53
STJO	0.54	0.38	1.62
SYOG	0.68	0.62	2.57
THTI	0.63	0.80	2.69
TLSE	0.42	0.35	1.35
USNO	0.45	0.46	1.50

**Table 2** Amplitudes of the annual signals in the components North, East and Up.

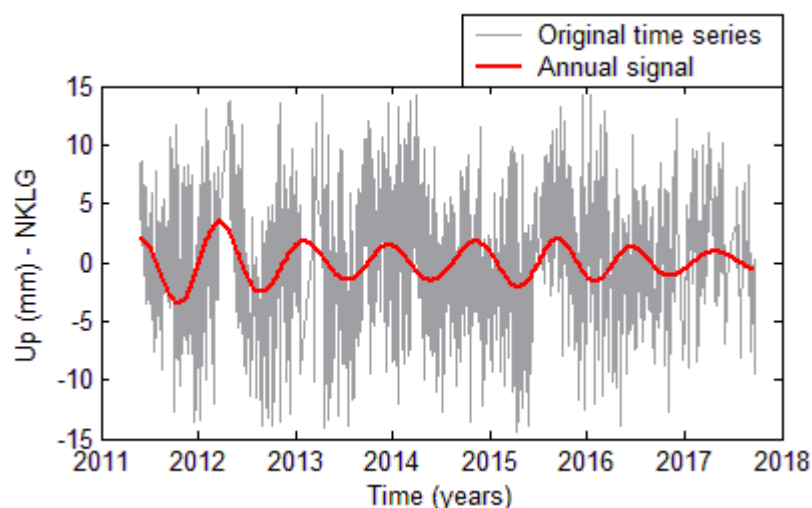


**Fig. 2.** Overlay of the Up component of the NKLK station with its annual signal (details 8) using discrete Meyer wavelet.

#### 4.2 Correlation between the GSP annual signal and the atmospheric and hydrological loading series

As discussed above, many studies (Petrov and Boy, 2004; Steigenberger et al., 2009; Eriksson and MacMillan, 2014) have shown the presence of atmospheric and hydrological pressure loading in position time series of space geodetic stations (VLBI, SLR, GPS and DORIS). For this fact, we have calculated the correlation between the GPS annual signal and the three-dimensional (North, East and Up) displacements caused by atmospheric and hydrological loading for each analyzed station.

The used atmospheric and hydrological loading time series are the three-dimensional (North, East and Up) displacements in millimeters for ITRF2014 sites. For atmospheric loading estimates, we used the ECMWF-IB (Wunsch and Stammer, 1997), ECMWF-TUGO-m barotropic (Carrère and Lyard, 2003) and ERA interim (Berrisford et al., 2011) models. For hydrological loading, we used the GLDAS/Noah (Rodell et al., 2004), ERA interim and MERRA2 (Gelaro et al., 2017) models.

Tables 3 and 4 give the correlations between the GPS annual signal and the atmospheric and hydrological loading displacement time series. The results reveal a low correlation between the GPS annual signal and the atmospheric and hydrological loading displacement time series for the three components North, East and Up. The results also show that the correlations per component for all stations are consistent between all atmospheric and hydrological models.

Stations	ECMWF-IB			ECMWF-TUGO-m barotropic			ERA interim		
	North	East	Up	North	East	Up	North	East	Up
GODE	-0.10	-0.01	-0.04	-0.12	-0.03	-0.11	-0.09	0	-0.08
KOKB	-0.16	0.09	0.13	-0.13	0.11	0.10	-0.15	0.07	0.13
METS	0.09	0.07	0.06	0.11	0.09	0.09	0.17	0.09	0.04
NKLG	-0.63	-0.07	0.11	-0.59	-0.02	0.11	-0.66	-0.09	0.15
NYA1	0	-0.09	0.03	0.03	-0.06	0.04	-0.01	-0.04	0
REYK	0.02	0	0.15	0.05	0.05	0.16	-0.07	-0.02	0.03
STJO	-0.01	-0.01	-0.04	-0.03	-0.02	-0.01	-0.05	0	-0.05
SYOG	0.13	0.16	0.15	0.15	0.21	0.23	0.14	0.06	0.13
THTI	0.03	0	-0.01	0.02	-0.01	-0.04	-0.02	-0.09	0.01
TLSE	-0.01	0.08	0.08	0.06	0	0.08	-0.01	0.08	0.08
USNO	-0.01	-0.08	-0.03	0.02	-0.06	-0.05	0.02	-0.05	-0.02

**Table 3** Correlation between the GPS annual signal and the atmospheric loading displacements estimated from ECMWF-IB, ECMWF-TUGO-m barotropic and ERA interim models, in the components North, East and Up.

Stations	GLDAS/Noah			ERA interim			MERRA2		
	North	East	Up	North	East	Up	North	East	Up
GODE	0.36	0.39	0.16	0.20	0.31	-0.30	0.32	0.42	0.06
KOKB	-0.10	-0.46	0.03	-0.16	-0.51	0.12	-0.11	-0.43	0.05
METS	-0.04	-0.05	0.15	0.07	-0.01	-0.09	0.01	-0.02	0.10
NKLG	-0.13	0.34	0.03	0.04	0.41	0.04	-0.24	0.36	0
NYA1	0.01	-0.11	0.06	0.07	-0.04	0	0.08	-0.02	0.03
REYK	0	-0.05	0.05	0.08	-0.05	0.01	-0.01	-0.03	-0.04
STJO	-0.24	0.01	0.03	-0.04	0.14	0.02	-0.02	0.11	0.03
SYOG	-0.09	-0.03	-0.10	0	0.05	-0.07	-0.04	-0.02	0.02
THTI	0.01	0.08	-0.13	-0.01	0.10	-0.11	0.06	0.06	-0.19
TLSE	0.02	-0.58	0.32	-0.03	-0.52	0.33	0	-0.56	0.28
USNO	-0.24	-0.06	-0.20	-0.16	-0.05	0.10	-0.14	-0.09	0.11

**Table 4** Correlation between the GPS annual signal and the hydrological loading displacements, estimated from GLDAS/Noah, ERA interim and MERRA2 models, in the components North, East and Up.

## 5. CONCLUSION

The main purpose of this paper was to study the correlation between the annual signal observed in GPS station position time series and the atmospheric and hydrological pressure loading signals. After having extracted the annual signal from the analyzed position time series with the multi-resolution analysis, we calculated the correlation between this annual signal and the three-dimensional (North, East and Up) displacements caused by atmospheric and hydrological loading.

The calculated correlation coefficients between the annual signal and the atmospheric loading estimated from ECMWF ECMWF-IB, ECMWF-TUGO-m barotropic and ERA interim models, and the hydrological loading estimated from GLDAS/Noah, ERA interim and MERRA2 models, show small (or negative) correlations in the three components (North, East and Up) for all analyzed stations.



## REFERENCES

- Altamimi, Z., Rebischung, P., Métivier, L., Collilieux, X., 2016. ITRF2014: A new release of the International Terrestrial Reference Frame modeling nonlinear station motions. *Journal of Geophysical Research: Solid Earth* 121(8), 6109–6131.
- Barlier, F., 2005. The DORIS system, A fully operational tracking system to get orbit determination at centimeter accuracy in support of Earth observations. *C. R. Geosci.* 337 (14), 1223–1224.
- Berrisford, P., Kallberg, P., Kobayashi, S., et al., 2011. Atmospheric conservation properties in ERA–Interim. *Quart. J. R. Meteorol. Soc.*, 137, 1381–1399.
- Carrère, L., Lyard, F., 2003. Modeling the barotropic response of the global ocean to atmospheric wind and pressure forcing – comparisons with observations. *Geophys. Res. Lett.* 30(6), 1275.
- Daubechies, I. Ten lectures on wavelets, 1992. Society for Industrial and Applied Mathematics (SIAM), USA, 357 pages.
- Dow, J.M., Neilan, R.E., Rizos, C., 2009. The International GNSS Service in a changing landscape of Global Satellite Navigation Systems. *J. Geod.* 83 (3–4), 191–198.
- Eriksson, D., MacMillan, D.S., 2014. Continental hydrology loading observed by VLBI measurements. *J. Geod.* 88:675–690.
- Gelaro, R., McCarty W., Suarez M.J., et al., 2017. The Modern–Era Retrospective Analysis for Research and Applications, Version 2 (MERRA–2). *Journal of Climate (J. Clim.)*, 30(14), 5419–5454.
- Khelifa, S., 2016. Noise in DORIS station position time series provided by IGN–JPL, INASAN and CNES–CLS Analysis Centres for the ITRF2014 realization. *Adv. Space Res.*, 58(12), 2572–2588.
- Mallat, S. A Wavelet Tour of Signal Processing (Second Edition), 1999. Academic Press, USA, 637 pages.
- Pearlman, M.R., Degnan, J.J., Bosworth, J.M., 2002. The International Laser Ranging Service. *Adv. Space Res.* 30(2), 135–143.
- Petrov, L., Boy, J. P., 2004. Study of the atmospheric pressure loading signal in very long baseline interferometry observations. *J. Geophys. Res.* 109(B3):B03405.

Rodell, M., Houser, P. R., Jambor, U., et al., 2004. The Global Land Data Assimilation System. *Bull. Amer. Meteor. Soc.* 85(3), 381–394.

Schuh, H., Behrend, D., 2012. VLBI: A fascinating technique for geodesy and astrometry. *J. Geodyn.* 61, 68–80.

Steigenberger, P., Boehm, J., Tesmer, V., 2009. Comparison of GMF/GPT with VMF1/ECMWF and implications for atmospheric loading. *J. Geod.* 83(10), 943–951.

Wunsch, C., Stammer, D., 1997. Atmospheric loading and the oceanic "inverted barometer" effect, *Rev. Geophys.*, 35, 79–107.

Zumberge, J.F., Heflin, M.B., Jefferson, D.C., Watkins, M.M., Webb, F.H., 1997. Precise point positioning for the efficient and robust analysis of GPS data from large networks. *J. Geophys. Res.* 102(B3), 5005–5017.

## **BIOGRAPHICAL NOTES**

**Dr. Sofiane KHELIFA** is a Research Master at the Department of Space Geodesy at the Centre of Space Techniques (Arzew/ALGERIA). His main area of interest is the analysis and diagnosis of position time series of space geodetic stations (VLBI, SLR, GPS and DORIS) in order to assess their systematic signals (trends and seasonal components) and their noise. On this research subject, he has presented papers at numerous international conferences and has published articles in various journals (Elsevier and Springer editions).

## **CONTACTS**

Dr. Sofiane KHELIFA  
Department of Space Geodesy / Centre of Space Techniques (CTS)  
PO Box 13, 31200  
Arzew  
ALGERIA  
Tel. +213 41472217  
Fax +213 41473665  
Email: [khelifa\\_sofiane@yahoo.fr](mailto:khelifa_sofiane@yahoo.fr)

---

Investigation of Atmospheric and Hydrological Loading Signals in the Annual Signal of GPS Station Positions (9375)  
Sofiane Khelifa (Algeria)

FIG Congress 2018

Embracing our smart world where the continents connect: enhancing the geospatial maturity of societies  
Istanbul, Turkey, May 6–11, 2018